의학박사 학위논문

Evaluation of Bipolar Radiofrequency Ablation of the Native and Stented Bile Duct

– In Vivo and In Vitro Study –

정상 담관과 금속 스텐트를 삽입한 담관에 대한 양극성 고주파 열치료 효과의 평가

2014 년 8 월

서울대학교 대학원

의학과 내과학전공

윤 원 재

의학박사 학위논문

Evaluation of Bipolar Radiofrequency Ablation of the Native and Stented Bile Duct

– In Vivo and In Vitro Study –

정상 담관과 금속 스텐트를 삽입한 담관에 대한 양극성 고주파 열치료 효과의 평가

2014 년 8 월

서울대학교 대학원

의학과 내과학전공

윤 원 재

정상 담관과 금속 스텐트를 삽입한 담관에 대한 양극성 고주파 열치료 효과의 평가

지도 교수 김 용 태

이 논문을 의학박사 학위논문으로 제출함
2014년 7월

서울대학교 대학원
의학과 내과학 전공
윤 원 재

윤원재의 의학박사 학위논문을 인준함
2014년 8월

위 원 장 _____ (인)
부위원장 _____ (인)
위 원 _____ (인)
위 원 _____ (인)
위 원 _____ (인)

Evaluation of Bipolar Radiofrequency Ablation of the Native and Stented Bile Duct

– In Vivo and In Vitro Study –

by

Won Jae Yoon

A thesis submitted to the Department of Medicine in partial fulfillment of the requirements for the Degree of Doctor of Philosophy in Medical Science (Internal Medicine) at Seoul National University College of Medicine

August 2014

Approved by Thesis Committee:

Professor _____**Chairman**

Professor _____**Vice chairman**

Professor _____

Professor _____

Professor _____

ABSTRACT

Evaluation of Bipolar Radiofrequency Ablation of the Native and Stented Bile Duct

− In Vivo and In Vitro Study −

Won Jae Yoon

Department of Medicine (Internal Medicine)

The Graduate School

Seoul National University

Introduction: Radiofrequency ablation (RFA) has been shown to be effective in the management of hepatocellular carcinoma and Barrett's esophagus with high-grade dysplasia. Recently, bipolar RFA catheters for endobiliary RFA have been introduced. RFA may prolong the survival of poor surgical candidates with extrahepatic cholangiocarcinoma. Furthermore, it may prolong the patency of self-expandable metal stents (SEMSs) which are used in the palliation of unresectable malignant biliary obstruction. The aims of this study was to determine the effect of endobiliary bipolar RFA in the native and stented porcine bile duct according to different power settings, and to simulate

the bipolar RFA effect on tissue ingrowth that causes SEMS occlusion using polyacrylamide gel phantom model.

Methods: Six farm pigs (3 for RFA of the native bile duct and 3 for the RFA of the stented bile duct) were used for this study. After a midline laparotomy and a duodenotomy, the bile duct opening was identified. For RFA of the native bile duct, a bipolar RFA catheter was placed through the bile duct lumen. RFA settings were 5 W (n=1), 7 W (n=1), and 10 W (n=1); the duration of RFA was 90 seconds. For the RFA of the stented bile duct, an uncovered SEMS was deployed in 3 pigs. The endobiliary RFA catheter was introduced through the lumen. The RFA setting was 10 W (n=3); the duration was 90 seconds. The bile duct was examined for histological changes. In vitro simulation of RFA of tissue ingrowth in SEMS was done using polyacrylamide gel phantom model. RFA at power of 10 W and duration of 30 seconds was done to uncovered SEMS-embedded and covered SEMS-embedded gel phantoms and plain gel phantoms serving as controls. The RFA effects were compared.

Results: In the native porcine bile duct, the depth of ablation was 0.9 ± 0.3, 1.5 ± 0.2, 2.3 ± 0.6 mm at 5, 7, and 10 W, respectively (analysis of variance; P = 0.02). There was a linear relationship between power and depth of ablation (r^2 = 0.78; P = 0.003). In the stented bile ducts, the ablated area was distributed along the area adjacent to the electrodes of the RFA probe. The depth of ablation was limited to the superficial mucosa at 10 W. The RFA of uncovered SEMS-embedded gel phantoms resulted in early termination of RF generation upon contact of the coagulated area with the wire of the SEMS. In

the damaged covered SEMS-embedded gel phantom model, early termination of RF generation was not observed. In half of the models, the coagulated area was confined within the covered SEMS lumen. In the other half, the coagulated area expanded beyond the wall of covered SEMS.

Conclusions: Application of bipolar RFA to patients with extrahepatic cholangiocarcinoma may be safe and feasible. However, bipolar RFA of tissue ingrowth in uncovered SEMS might be of limited efficacy, as the RFA effect is limited around the individual electrodes and cannot reach beyond the SEMS wall. Bipolar RFA of tissue ingrowth in covered SEMS might be of more efficacy, as the RFA effect may reach beyond the wall of SEMS.

* The results of native porcine bile duct RFA in this thesis was published in: Daglilar ES, Yoon WJ, Mino-Kenudson M, Brugge WR. Controlled swine bile duct ablation with a bipolar radiofrequency catheter. Gastrointest Endosc. 2013;77(5):815-9.

Keywords: Catheter ablation, Bile ducts, Swine, Metal stent

***Student Number*: 2006-30512**

CONTENTS

LIST OF TABLES AND FIGURES

LIST OF ABBREVIATIONS

EHC: extrahepatic cholangiocarcinoma

PDT: photodynamic therapy

RF: radiofrequency

RFA: radiofrequency ablation

SEMS: self-expandable metal stent

INTRODUCTION

Extrahepatic cholangiocarcinoma (EHC) accounts for 0.16% of all invasive cancers in males and 0.15% in females in the general population (1). In Korea, where the incidence of EHC of somewhat higher, the mean incidence of EHC between 2002 and 2006 was 5.1 per 100,000 persons (2). Surgical resection remains to be the choice of treatment. Five-year survival rates after complete resection of EHC ranges from 11% to 41%, depending on the location of the cancer. However, complete resection is achieved in less than 50% of the cases (3).

Resection for EHC almost invariably involves extensive surgery. When the cancer involves the proximal third of the extrahepatic bile duct, then resection of the bile duct, adjacent liver and lymph nodes is carried out. When the cancer involves the middle third of the extrahepatic bile duct, resection of the bile duct and lymph node is warranted. When the distal third of the extrahepatic bile duct is involved with cancer, a pancreaticoduodenectomy is performed (4). Although the incidence of surgical complications has decreased over time, the elderly and the premorbid patients may not tolerate the surgical procedures. The mortality rate of pancreaticoduodenectomy ranges from 1 to 3.9%; the incidence of pancreatic fistula, the most dreaded complication after pancreaticoduodenectomy, ranges from 2.1 to 12.6% (5). Therefore, a less invasive treatment option may be feasible for patients who are poor candidates for surgery.

For those who are poor candidates of surgery, chemotherapy or photodynamic therapy (PDT) may be offered. In the recently published,

randomized, controlled phase III study, the combination of gemcitabine and cisplatin improved overall and progression-free survival by 30% over gemcitabine alone in patients with locally advanced or metastatic cholangiocarcinoma, gallbladder cancer, or ampullary cancer (6).

PDT is an ablative therapy which involves injection of a photosensitizer and irradiation of the tumor with light of a specific wavelength. In small randomized clinical trials, the combination of PDT with biliary stenting resulted in improvement of overall survival of patients with unresectable cholangiocarcinoma (7, 8). However, photosensitizer must be administered before PDT. In addition, the photosensitizer may result in photosensitivity. Some advocate protection from direct sunlight or bright indoor light for 2 months (9).

Radiofrequency ablation (RFA) may offer another option of ablative therapy for EHC. Recently, bipolar RFA catheters for endobiliary RFA have been introduced. During RFA, electrical current from the generator oscillates between electrodes through ion channels present in tissues. As the tissues are imperfect conductors of electricity, the flow of the electrical current results in friction agitation at the ionic level and heat generation (Joule effect). Tissues nearest to an electrode are heated most effectively; more peripheral areas of tissues receive heat by thermal conduction (10). RFA has been used to treat hepatocellular carcinoma (11, 12) and Barrett's esophagus with high-grade dysplasia (13).

Self-expandable metal stents (SEMSs) are used in the palliation of unresectable malignant biliary obstruction. They offer longer patency

compared to plastic stents (14-18). However, SEMSs may become occluded in some patients, mostly due to tissue ingrowth (18, 19). Only a limited number of reports are available on the management of occluded SEMSs. Current management of occluded SEMSs includes insertion of additional stents or percutaneous transhepatic biliary drainage (20-25). However, none of the approaches target the tumor itself. Development of a therapeutic approach targeting the tumor may result in prolongation of stent patency. In addition to its potential usefulness in the ablative therapy for EHC, RFA may be used in the management of SEMS occlusion, especially when due to tissue ingrowth. A pre-emptive RFA done prior to SEMS insertion might prolong its patency. Furthermore, this may prolong patient survival, especially in poor surgical candidates who, despite localized disease, cannot tolerate a pancreaticoduodenectomy and ultimately undergo SEMS insertion.

The evaluation of the depth of ablation according to various power settings in the in vivo bile duct using this bipolar RFA catheter is critical, as it will be the first step in the determination of the utility of such device. The presence of SEMS may affect the depth of RFA of the tissue beyond the SEMS. What might be more important than the effect on the depth, however, is the effect of the SEMS on the long axis of the RFA. In detail, if the SEMS conduct the thermal energy to a certain degree, the presence of the SEMS may result in unnecessary ablation of the portion of the bile duct that is not cancerous.

Review of the literature reveals lack of experience in application of bipolar RFA in the bile duct in vivo. Furthermore, there is no previous study

on the effect of bipolar RFA in the bile duct with a SEMS inserted.

The aims of this study were (1) to determine the depth of bipolar endobiliary RFA in the native porcine bile duct according to different power settings, (2) determine the performance characteristics of endobiliary RFA in the stented porcine bile duct, and (3) to see if the presence of a SEMS has any effect on the conduction of energy when radiofrequency (RF) is applied to ingrown tissue using an in vitro and ex vivo model.

The results of native porcine bile duct RFA in this thesis was published in 2013, coauthored by Ebubekir S. Daglilar, Won Jae Yoon, Mari Mino-Kenudson, and William R. Brugge (26). My role as the coauthor was conducting the animal experiment, acquisition, analysis, and interpretation of the data.

MATERIALS AND METHODS

Animal procedures

This study was approved by the Massachusetts General Hospital Subcommittee on Research Animal Care. Six farm pigs (3 for RFA of the native bile duct and 3 for the RFA of the stented bile duct) weighing 40 – 50 kg were used for this study. The animals were provided with liquid diet on Day -2 and Day -1. Food was withheld from the animals from the midnight of Day 0 until the induction of anesthesia.

All animals underwent general anesthesia with induction by telazol/xylazine 4.4 mg/kg IM + 2.2 mg/kg IM. The animals were intubated immediately and isoflurane anesthesia (1.5 – 3.0%) with oxygen supplementation (3.0 L/min) was given. A ground pad for electrosurgical unit was applied to the skin of a hind leg of the animal.

RF power was generated using 50/60 Hz, ERBE VIO® 300D electrosurgical generator (ERBE USA Inc., Marietta, GA, USA). The Habib™ EndoHPB catheter (Figure 1) was used to deliver RF energy to the porcine bile duct.

a. RFA of the native bile duct (n=3)

Following general anesthesia, a midline laparotomy was made. After the incision, the duodenum was identified and an incision was made on the duodenum to expose the lumen. The duodenal mucosa was searched for the bile duct opening. Once the bile duct opening had been identified, the RFA catheter was inserted to the bile duct in a retrograde fashion. The RFA was

done at the power settings of 5 W (n=1), 7 W (n=1), and 10 W (n=1) and duration of 90 seconds. For each porcine bile duct, RFAs were done to 3 sites: proximal, middle, and distal bile duct.

b. RFA of the stented bile duct (n=3)

The laparotomy, duodenotomy, and identification of the bile duct opening were done in the same fashion as described previously.

After identification of the bile duct opening, a 10-mm × 6-cm uncovered SEMS (Zilver® stent, Cook Medical, Winston-Salem, NC, USA) was inserted and deployed. After the deployment of the SEMS, the bile duct wall was compressed manually to facilitate tissue embedding in the mesh of the stent. The RFA catheter was inserted into the stent lumen, and then the bile duct was loosely tied in the middle portion to simulate a biliary stricture. RFA was done at the power setting of 10 W and duration of 90 seconds (n=3). For each stented porcine bile duct, RFA was done to a single site.

Histological evaluation

After the completion of the study, the animals were euthanized by pentobarbital overdose. Necropsy was done to harvest the bile duct. Specimens were fixed in 10 % formalin. The specimens were sent for pathological evaluation for the depth of coagulative tissue necrosis.

In vitro model of bipolar RFA of tissue ingrowth in SEMS

No in vivo model is available to simulate the tissue ingrowth through the mesh of SEMS in malignant biliary obstruction. Therefore, an in vitro model using polyacrylamide gel phantom was carried out.

Polyacrylamide gel was made by modifying the recipe developed by McDonald (27) and Bu-Lin (28). The recipe is described in Table 1. The fluid was poured into 4-mL, cuboidal cuvettes (Ratiolab, Dreieich, Germany). RF was delivered using ELRA electrode (Figure 2) and VIVA RF generator (STARmed, Gyeonggi-do, Korea). The power was set at 10 W. The duration of RFA that resulted in the optimal RFA depth of the model was determined in the plain gel phantoms (i.e., gel phantoms without SEMS embedded).

The in vitro tissue ingrowth model was developed for both uncovered and covered SEMS. For uncovered SEMS, 10 gel phantom models were embedded with 6-mm, 3-cm uncovered SEMSs (Hanarostent® Biliary, MI Tech, Seoul, Korea). For covered SEMS, 10 gel phantoms were embedded with 8-mm, 3-cm covered SEMSs (Hanarostent® Biliary, MI Tech, Seoul, Korea). Prior to embedding, the covering membrane was punctured through every interstice. This was done to simulate tissue ingrowth through the damaged covering membrane. The ELRA electrode was introduced in to the SEMS lumen, and RFA was performed with the same power and duration.

The maximum length of short axis and the long axis were measured. The cross-sectional area of the coagulated area was calculated using the formula for the area of an ellipse: $\pi \times$ (long radius) $\times$ (short radius).

Ex vivo model of bipolar RFA of tissue ingrowth in SEMS

To further evaluate the bipolar RFA of tissue ingrowth in SEMS, ex vivo study using freshly resected bovine liver was carried out. To establish an ex vivo model, various methods including deployment of the SEMS with conventional delivery system in the liver parenchyma, improvisation of a hollow cylindrical SEMS delivery system, and sandwiching a SEMS between 2 pieces of liver tissue were tried.

Statistics

Values were shown as mean ± standard deviation. The linear regression analysis was used to show relationships between power and depth of ablation in the animal study. The cross-sectional areas of the coagulation of the gel phantom models were compared using the *t* test. A P value < 0.05 was considered significant. Statistical analysis was performed using STATA 12.1 (StataCorp LP, College Station, TX, USA).

RESULTS

RFA of the native porcine bile duct

In the study animals, RF power was applied to the bile duct without difficulty. Sites of ablation in the bile duct were evident grossly and histologically. The depth of coagulative necrosis in the bile duct was 0.9 ± 0.3, 1.5 ± 0.2, 2.3 ± 0.6 mm at 5, 7, and 10 W, respectively (analysis of variance; P = 0.02). There was a linear relationship between power and depth of ablation (r^2 = 0.78; P = 0.003) (Figure 3). At 5 W, ablation involved only the mucosa and epithelial glandular cells. At 7 W, ablation was limited to the bile duct wall, and the coagulative necrosis extended into the mucosa, glandular epithelial cells, and fibromuscular layer. At 10 W, ablation was transmural and reached beyond the bile duct wall and resulted in necrosis of surrounding pancreatic tissues and adjacent blood vessels (Figure 4).

RFA of the stented porcine bile duct

The deployment of the SEMS and the retrograde insertion of the endobiliary RFA catheter through the stent lumen were easily achieved in the 3 pigs.

Grossly, the ablated area was distributed only along the area adjacent to the electrodes of the RFA probe in 2 of the 3 pigs (Figure 5). In one pig, no gross change was noted. However, histology revealed that the ablative changes were distributed along the area adjacent to the electrodes.

In the stented bile duct, the depth of ablation was reduced compared to that of the unstented bile duct. In detail, the ablation was limited to the

superficial mucosa (Figure 6).

In vitro evaluation of bipolar RFA of tissue ingrowth in SEMS

The optimal RF setting for in vitro evaluation of bipolar RFA using the plain gel phantom was 10 W, temperature range of 65 – 75°C, with duration of 30 seconds. This setting resulted in an ovoid coagulated area with mean short axis of 9.1 ± 0.2 mm and long axis of 11.8 ± 1.1 mm (n=10). The short axis of the coagulated area just reached the wall of the cuvette (Figure 7A). The mean cross-sectional area of coagulation was 84.3 ± 7.4 mm^2.

Bipolar RFA of the uncovered SEMS-embedded gel phantom model resulted in early termination of RF generation. In detail, during the early course of RFA, a rapid drop in the impedance of the circuit was observed when the coagulated area came into contact with the wire of the uncovered SEMS. Subsequently the generation of RF was terminated, and re-initiation of RF generation was not possible. This phenomenon was observed in all 10 uncovered SEMS-embedded gel phantoms. Only small areas of coagulation confined near to individual electrodes were observed (Figure 7B). The mean cross-sectional area of coagulation was 16.2 ± 11.0 mm^2, which was significantly different when compared to that of the plain gel phantoms ($P < 0.001$).

Bipolar RFA of the damaged covered SEMS-embedded gel phantom model resulted in an ovoid area of coagulation. No early termination of RF

generation was observed. In 5 models, the coagulated area was confined within the SEMS lumen (Figure 7C). In the other 5 models, the coagulated area expanded beyond the wall of SEMS (Figure 7D). The mean cross-sectional area of coagulation of 10 gel phantoms was 73.0 ± 14.9 mm^2. There was statistically significant difference between the mean areas of coagulation of plain gel phantoms and damaged covered SEMS-embedded gel phantoms ($P = 0.047$).

To further evaluate the effect of the presence of covering membrane of the covered SEMS on bipolar RFA, bipolar RFA of undamaged covered SEMS-embedded gel phantom model was carried out (n=10). This resulted in an ovoid area of coagulation within the stent lumen only. No early termination of the RF generation was observed. The covering material of the stent remained intact after RFA. This phenomenon was observed in all 10 gel phantom models (Figure 7E). The mean cross-sectional area of coagulation of 10 gel phantoms was 53.2 ± 5.5 mm^2. There was statistically significant difference between the mean areas of coagulation of plain gel phantoms and intact covered SEMS-embedded gel phantoms ($P < 0.001$).

Trial of ex vivo evaluation of bipolar RFA of tissue ingrowth in SEMS

Establishing a robust ex vivo model was not possible. When using a conventional delivery system, the SEMS did not expand immediately, which is a matter of course. Improvised SEMS delivery system resulted in excessive

space in the liver tissue, and the liver tissue within the SEMS lumen was not fixed. Insertion of RFA catheter into the intraluminal liver tissue was not possible. The liver tissue did not embed enough into the lumen of the SEMS when the sandwich method was used.

DISCUSSION

The purpose of this study was to provide preliminary data for the use of the bipolar endobiliary RFA. In the native porcine bile duct, bipolar RFA resulted in ablation of the bile duct wall with a linear relationship between the depth of coagulative necrosis and the RF power. In the porcine bile duct with a SEMS in place, the retrograde insertion of the RFA catheter through the SEMS lumen was easily achieved. The area of coagulative necrosis was distributed only along the area adjacent to the electrodes of the bipolar RFA probe, and not throughout the entire length of the SEMS. However, the depth of coagulative necrosis was reduced in the stented porcine bile duct. In vitro model of bipolar RFA of tissue ingrowth in SEMS showed different results between uncovered and covered SEMS. In the uncovered SEMS-embedded gel phantom model, early termination of RF generation was observed resulting in limited coagulation. In the damaged covered SEMS-embedded gel phantom model, no early termination of RF generation was seen. In 50% of the models, the coagulated area was confined within the covered SEMS lumen. In the other 50%, the coagulated area expanded beyond the wall of covered SEMS. In all the intact covered SEMS-embedded gel phantom models, the coagulated area was confined within the SEMS lumen. When compared to that of plain gel phantom models, the cross-sectional areas of coagulation of the SEMS-embedded models were significantly smaller.

There is one report on the effects of Habib^{TM} EndoHPB catheter using an ex vivo pig liver. In this study, the RF was applied step by step at 5, 10, 15, and 20 W of power and 60, 90, and 120 seconds, respectively. The mean

lengths of the short axis of the ablated area at 10 W and 60, 90, and 120 seconds were 8.0 ± 1.0, 8.3 ± 1.2, and 9.7 ± 0.6 mm, respectively. The mean lengths of the long axis at corresponding settings were 20.3 ± 0.6, 21.3 ± 1.6, and 28.3 ± 2.1 mm, respectively. The lengths of the short and long axes at 5 and 10 W increased with power; no obvious differences in axes lengths between 15 and 20 W were noted (29). However, it must be emphasized that this is the result of the RFA of ex vivo porcine liver parenchyma.

Endobiliary RFA has been shown to be safe and feasible. In a phase I study involving 22 subjects with unresectable malignant biliary obstruction, deployment of the Habib^{TM} EndoHPB catheter under endoscopic retrograde cholangiographic guidance was successful in 21 patients. Asymptomatic biochemical pancreatitis developed in 1 patient. Two patients developed cholecystitis requiring percutaneous gallbladder drainage. 1 patient developed rigors that resolved after antibiotic therapy. The reported complications were similar with regard to type and incidence for deployment of biliary metal stent insertion (30). The RF power was generated by using a setting of 7 or 10 W delivered over 2 minutes. However, the depth, extent, and degree of tissue ablation could not be assessed in the study.

The results of the RFA of the native porcine bile duct indicate that bipolar RFA provides various degree of ablation according to the power. At 10 W, transmural ablation was observed. Endobiliary RFA may result in transmural injury and possibly bile duct perforation at high powers.

The presence of SEMS in the porcine bile duct was associated with markedly reduced RFA depth. This shows that the application of bipolar RF

within the lumen of SEMS induces ablation with characteristics that are different from those of monopolar RFA. Goldberg et al (31) demonstrated that application of monopolar RFA on the SEMS result in circumferential coagulative necrosis of the surrounding tissue along the entire SEMS length. In that study, monopolar RF was applied to the SEMS itself placed in the porcine hepatic veins. This resulted in 8 – 10 mm of uniform circumferential coagulative necrosis along the SEMS length (31).

Bipolar RFA of the uncovered SEMS-embedded gel phantom model resulted in early termination of RF generation. In this model, as the coagulated area came into contact with the wire of the SEMS, a rapid reduction of the impedance of the circuit was observed. When the current flows through the wire of the uncovered SEMS, there is a rapid decrease in the impedance between the RFA electrodes. When the impedance between the RFA electrodes is greater than that of the generator, heat is generated in the electrodes. However, when the impedance of RFA electrodes is lower than that of the generator, the generator starts to generate heat. When the impedance between the RFA electrodes becomes lower than the preset impedance, the generator is shut off to protect itself from overheating. It is known that the power is shut off when the bipolar RFA electrodes contact the SEMS (32). However, current result strongly suggests that the electrodes need not be in direct contact with the SEMS for the power to be shut off. Also, current result suggests that RFA effect to the peripheral areas of tissues is induced by passage of current in addition to thermal conduction. If the RFA effect in the peripheral areas are due solely to heat conduction, current

observation could not have occurred. One can speculate that when performing RFA in occluded uncovered SEMS due to tissue ingrowth, multiple repositioning may be necessary to achieve adequate ablation.

Bipolar RFA of the covered SEMS-embedded gel phantom model did not result in early termination of RF generation. As the covering membrane is located inside the stent, the current does not contact the metal wire of the SEMS. Therefore, no early termination of RF generation occurs. In half of covered SEMS-embedded gel phantoms, coagulation beyond the wall of SEMS was observed. This is most likely due to conduction of heat through the holes made to the covering membrane. Indeed, bipolar RFA of undamaged covered SEMS-embedded gel phantom models resulted in coagulation of gel confined to the stent lumen only.

Limitations of this study include use of a normal animal model, and manual placement of both SEMS and the RFA catheter. As there is no animal model of biliary stricture available yet, in vitro models were used to simulate tissue ingrowth in SEMS. An ex vivo model of tissue ingrowth could not be developed.

Current study results suggest that although higher power may be feasible to ablate cancerous tissue in the bile duct, power setting must be done with caution when RFA involves the margin of the cancer. The bile duct not affected by the cancer may receive excessive thermal injury which may result in bile duct perforation or unwanted damage of the adjacent tissue. It is likely that RFA of tissue ingrowth in uncovered SEMS would require multiple repositioning of the RFA catheter, as the incorporation of the exposed wire of

the uncovered SEMS into the circuit would shut down the generator. RFA of tissue ingrowth in covered SEMS, which is a rare event, might be easier, as early shut-off RFA generation is not likely to occur, and RFA effect may be maintained within the SEMS lumen or similar to that of unstented bile duct. Based on these results, human pilot study, followed by a randomized controlled trial is needed.

1. Dissolve 19.11 g of citric acid anhydrous (Sigma-Aldrich, C 0759) and 29.57 g sodium citrate tribasic dehydrate (Sigma-Aldrich, C 4641) in 166.67 mL of deionized water.
2. Gradually add 20 g of bovine serum albumin (Sigma-Aldrich, A4503) and 333.33 mL of 30%, 19:1 mixture of acrylamide and bis-acrylamide solution (Bio-Rad, 161-0154) and stir gently and not rapidly until the solution is homogeneous. Add deionized water if necessary (< 400 mL).
3. Add 60 mL of glycerol (99% w/v, Sigma-Aldrich, G5516-500ML) to the solution and stir gently until the solution is homogeneous.
4. Top up solution with deionized water to 1.0 L.
5. Dissolve into solution:
    (a) 1.00 g L-ascorbic acid (Sigma-Aldrich, A 5960)
    (b) 2.5 mL iron (II) sulfate heptahydrate ($FeSO_4$) (from a suspension of 1.00 g $FeSO_4$ in 100.0 mL of deionized water) (Sigma-Aldrich, F 7002)
    (c) 3.0 mL of 3.0% v/v hydrogen peroxide (H_2O_2) (dilution of 30% w/v stock, Sigma-Aldrich, H 1009)
6. Pour the solution immediately into the phantom mold avoiding air bubbles, seal and refrigerate. Although polymerization begins to occur in minutes, depending on the formulation, phantoms should remain refrigerated for a number of hours to preclude premature coagulation (e.g., a 50-mL sample is refrigerated for ≈ 1 hour). Refrigerated phantoms remain stable for several weeks, both before and after heating.

Table 1. Modified recipe for gel phantom with a citrate buffer concentration of 0.2 M and pH of 4.5 (1 L) according to McDonald et al (2004) and Bu-Lin et al (2008).

Figure 1. Habib™ EndoHPB bipolar radiofrequency ablation catheter.

Figure 2. ELRA bipolar radiofrequency ablation catheter.

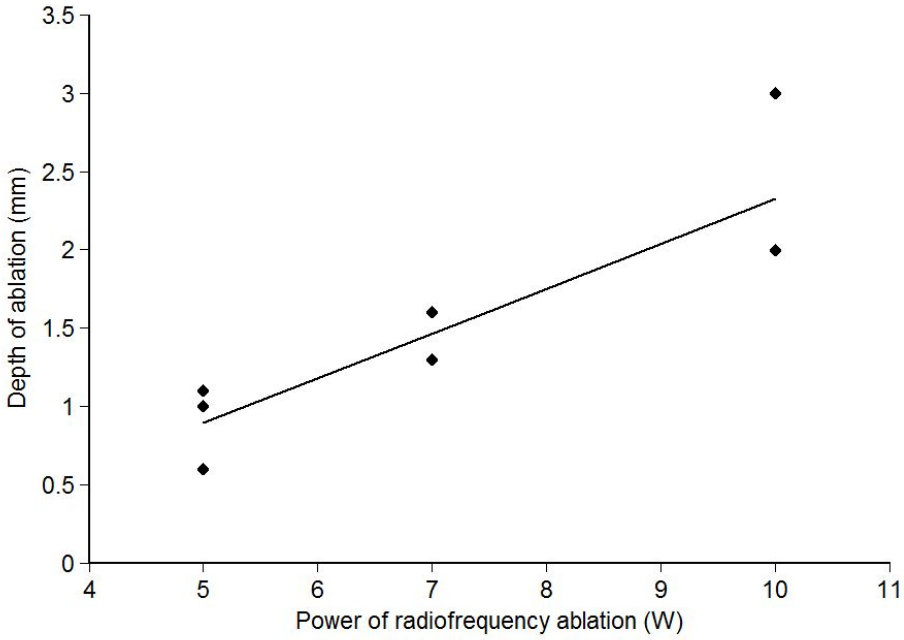

Figure 3. Linear relationship of power (W) and depth (mm) of ablation in the porcine bile duct (n=8, r^2 = 0.78; P = 0.003). At 7 W, 2 sites of ablation were noted. At 10 W, the depth of ablation was 3 mm in one site and 2 mm in the other 2 sites.

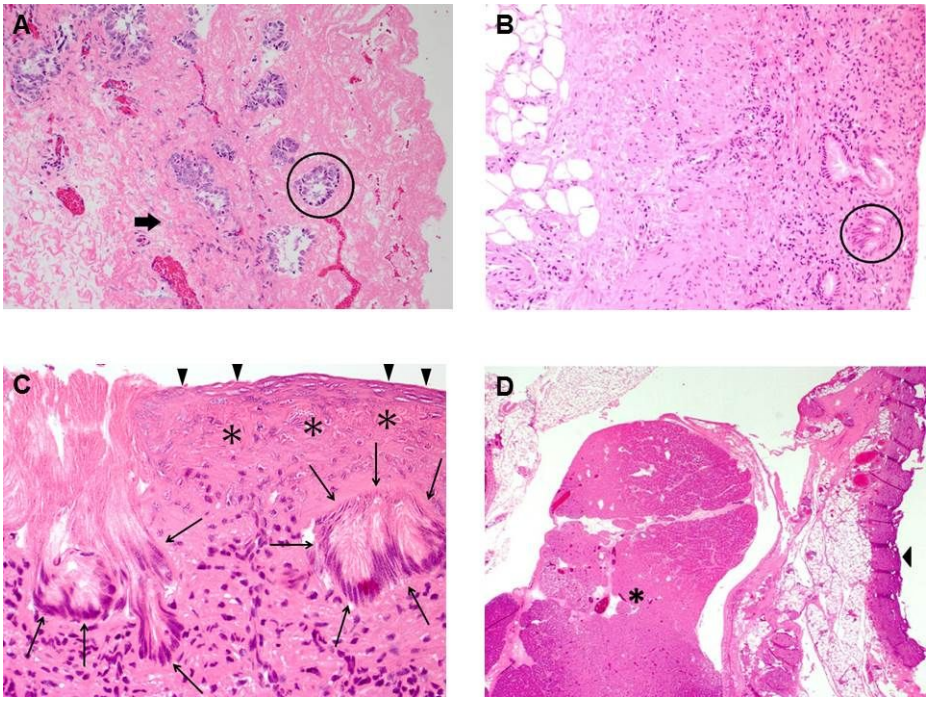

Figure 4. Histologic images of the porcine bile duct after radiofrequency ablation.

(**A**) At 5 W, coagulative necrosis was limited to the mucosal layer of the bile duct. Glandular epithelial cells appear viable (circle). Muscular layer was preserved (arrow) (H&E, orig. mag. ×200). (**B**) At 7 W, coagulative necrosis was confined to the bile duct gland wall (circle shows ablated glandular cells) (H&E, orig. mag. ×200). (**C**) At 10 W, note the absence of surface epithelium (arrowheads) and marked cautery effects involving deep glands (arrows) as well as stroma (asterisk) (H&E, orig. mag. ×400). (**D**) At 10 W, coagulative necrosis was transmural (arrowhead shows luminal side of bile duct). Histologic changes were seen in surrounding pancreatic tissue (asterisks) (H&E, orig. mag. ×20).

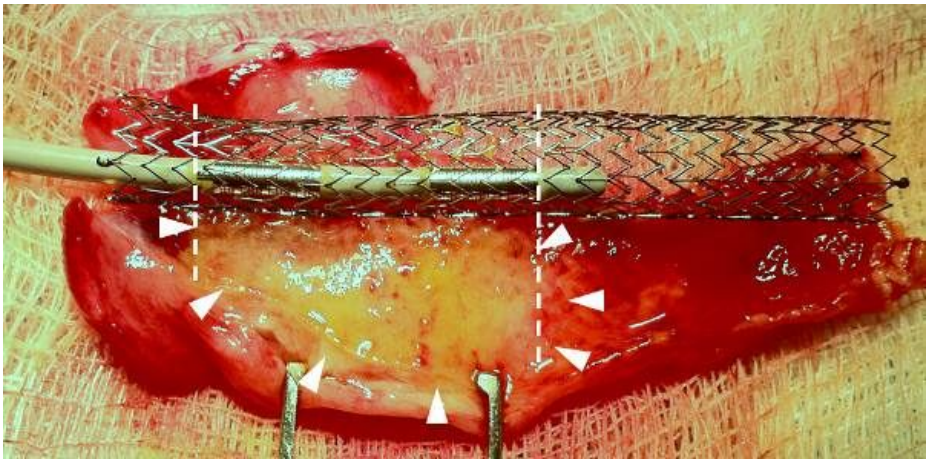

Figure 5. Gross photograph of the resected porcine bile duct specimen showing the relationship of the radiofrequency ablation catheter, self-expandable metal stent, and the ablated area of the bile duct wall.

The ablated mucosa has yellowish-tan color (arrowheads). The length of the ablated bile duct wall approximately matches the length between the two electrodes, demarcated by two dotted lines.

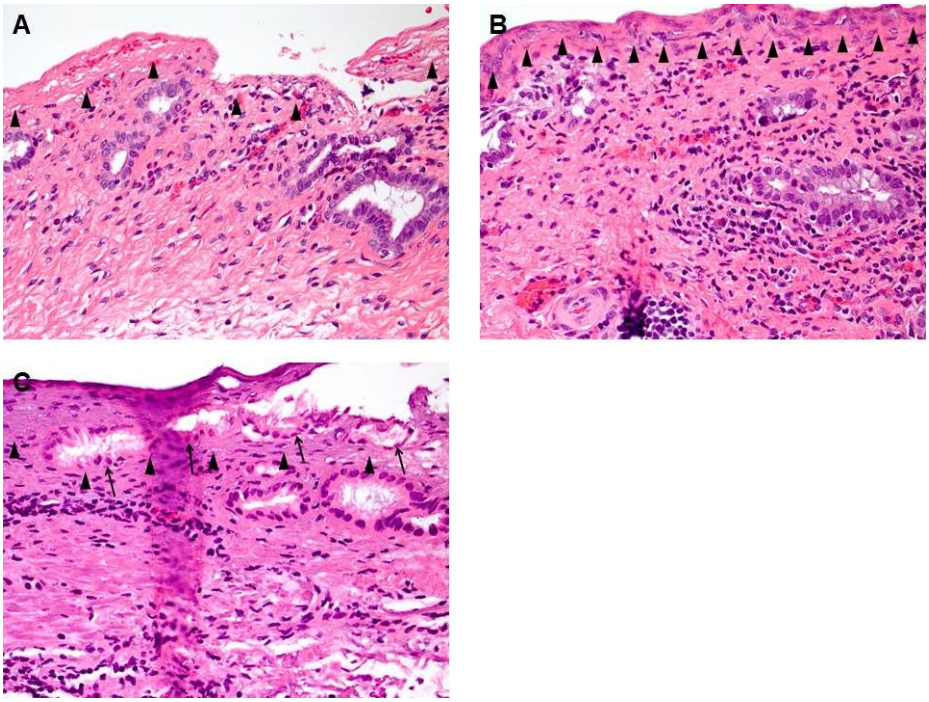

Figure 6. Photomicrograph of the stented porcine bile duct wall after RFA (H&E, orig. mag. ×400).

The depth of ablation was reduced compared to that of the of the unstented bile duct. (**A**), (**B**) The ablation of the surface mucosa (arrowheads) with preserved morphology of the deep glands is noted. (**C**) Ablation of the superficial mucosa (arrowheads) including glands limited to the superficial mucosal layer (arrows) is noted.


A


B


C


D


E

Figure 7. Representative photographs of bipolar RFA of gel phantom model.

(A) Bipolar RFA of gel phantom without SEMS. Note the ovoid area of coagulation. **(B)** Bipolar RFA of gel phantom with uncovered SEMS embedded. As the coagulated area contacted the wire of the uncovered SEMS, a rapid drop in the impedance, followed by immediate termination of RF generation was observed. Notice the small areas of coagulation confined near to individual electrodes. **(C)** Bipolar RFA of gel phantom with damaged covered SEMS embedded. In half of the models, the coagulation was confined within the lumen of SEMS. However, no early termination of RF generation was observed. **(D)** In the other half of the covered SEMS-embedded gel phantom model, the coagulated area expanded beyond the wall of SEMS. **(E)** Bipolar RFA of gel phantom embedded with undamaged covered SEMS. In all models, the coagulation was confined within the SEMS lumen.

REFERENCES

1. Albores-Saavedra J, Adsay NV, Crawford JM, Klimstra DS, Kloppel G, Sripa G, et al. Carcinoma of the gallbladder and extrahepatic bile ducts. In: Bosman FT, Carneiro F, Hruban RH, Theise ND, editors. WHO classification of tumours of the digestive system, 4th Ed. Lyon: IARC; 2010. p. 266-73.
2. Ryu JK. The epidemiology and risk factors of hilar cholangiocarcinoma. Korean J Med. 2010;79:593-6.
3. Feldman M, Friedman LS, Brandt LJ, editors. Sleisenger and Fordtran's gastrointestinal and liver disease: pathophysiology, diagnosis, and management. 9th Ed. Philadelphia: Saunders Elsevier; 2010. p.1171-84.
4. Sreenarasimhaiah J. Interventional endoscopic ultrasound: the next frontier in gastrointestinal endoscopy. Am J Med Sci. 2009;338(4):319-24.
5. Feldman M, Friedman LS, Brandt LJ, editors. Sleisenger and Fordtran's gastrointestinal and liver disease: pathophysiology, diagnosis, and management. 9th Ed. Philadelphia: Saunders Elsevier; 2010. p.1017-34.
6. Valle J, Wasan H, Palmer DH, Cunningham D, Anthoney A, Maraveyas A, et al. Cisplatin plus gemcitabine versus gemcitabine for biliary tract cancer. N Engl J Med. 2010;362(14):1273-81.
7. Ortner ME, Caca K, Berr F, Liebetruth J, Mansmann U, Huster D, et al. Successful photodynamic therapy for nonresectable cholangiocarcinoma: a randomized prospective study. Gastroenterology. 2003;125(5):1355-63.

8. Zoepf T, Jakobs R, Arnold JC, Apel D, Riemann JF. Palliation of nonresectable bile duct cancer: improved survival after photodynamic therapy. Am J Gastroenterol. 2005;100(11):2426-30.
9. Ortner MA, Dorta G. Technology insight: Photodynamic therapy for cholangiocarcinoma. Nat Clin Pract Gastroenterol Hepatol. 2006;3(8):459-67.
10. Ahmed M, Brace CL, Lee FT, Goldberg SN. Principles of and advances in percutaneous ablation. Radiology. 2011;258(2):351-69.
11. Sutherland LM, Williams JA, Padbury RT, Gotley DC, Stokes B, Maddern GJ. Radiofrequency ablation of liver tumors: a systematic review. Arch Surg. 2006;141(2):181-90.
12. Cho YK, Kim JK, Kim MY, Rhim H, Han JK. Systematic review of randomized trials for hepatocellular carcinoma treated with percutaneous ablation therapies. Hepatology. 2009;49(2):453-9.
13. Spechler SJ, Sharma P, Souza RF, Inadomi JM, Shaheen NJ. American Gastroenterological Association medical position statement on the management of Barrett's esophagus. Gastroenterology. 2011;140(3):1084-91.
14. Huibregtse K, Carr-Locke DL, Cremer M, Domschke W, Fockens P, Foerster E, et al. Biliary stent occlusion--a problem solved with self-expanding metal stents? European Wallstent Study Group. Endoscopy. 1992;24(5):391-4.
15. Davids PH, Groen AK, Rauws EA, Tytgat GN, Huibregtse K. Randomised trial of self-expanding metal stents versus polyethylene

stents for distal malignant biliary obstruction. Lancet. 1992;340(8834-8835):1488-92.

16. Knyrim K, Wagner HJ, Pausch J, Vakil N. A prospective, randomized, controlled trial of metal stents for malignant obstruction of the common bile duct. Endoscopy. 1993;25(3):207-12.
17. Rossi P, Bezzi M, Rossi M, Adam A, Chetty N, Roddie ME, et al. Metallic stents in malignant biliary obstruction: results of a multicenter European study of 240 patients. J Vasc Interv Radiol. 1994;5(2):279-85.
18. O'Brien S, Hatfield AR, Craig PI, Williams SP. A three year follow up of self expanding metal stents in the endoscopic palliation of longterm survivors with malignant biliary obstruction. Gut. 1995;36(4):618-21.
19. Schmassmann A, von Gunten E, Knuchel J, Scheurer U, Fehr HF, Halter F. Wallstents versus plastic stents in malignant biliary obstruction: effects of stent patency of the first and second stent on patient compliance and survival. Am J Gastroenterol. 1996;91(4):654-9.
20. Tham TC, Carr-Locke DL, Vandervoort J, Wong RC, Lichtenstein DR, Van Dam J, et al. Management of occluded biliary Wallstents. Gut. 1998;42(5):703-7.
21. Bueno JT, Gerdes H, Kurtz RC. Endoscopic management of occluded biliary Wallstents: a cancer center experience. Gastrointest Endosc. 2003;58(6):879-84.
22. Rogart JN, Boghos A, Rossi F, Al-Hashem H, Siddiqui UD, Jamidar P, et al. Analysis of endoscopic management of occluded metal biliary

stents at a single tertiary care center. Gastrointest Endosc. 2008;68(4):676-82.

23. Togawa O, Kawabe T, Isayama H, Nakai Y, Sasaki T, Arizumi T, et al. Management of occluded uncovered metallic stents in patients with malignant distal biliary obstructions using covered metallic stents. J Clin Gastroenterol. 2008;42(5):546-9.
24. Yoon WJ, Ryu JK, Lee JW, Ahn DW, Kim YT, Yoon YB, et al. Endoscopic management of occluded metal biliary stents: metal versus 10F plastic stents. World J Gastroenterol. 2010;16(42):5347-52.
25. Ridtitid W, Rerknimitr R, Janchai A, Kongkam P, Treeprasertsuk S, Kullavanijaya P. Outcome of second interventions for occluded metallic stents in patients with malignant biliary obstruction. Surg Endosc. 2010;24(9):2216-20.
26. Daglilar ES, Yoon WJ, Mino-Kenudson M, Brugge WR. Controlled swine bile duct ablation with a bipolar radiofrequency catheter. Gastrointest Endosc. 2013;77(5):815-9.
27. McDonald M, Lochhead S, Chopra R, Bronskill MJ. Multi-modality tissue-mimicking phantom for thermal therapy. Phys Med Biol. 2004;49(13):2767-78.
28. Bu-Lin Z, Bing H, Sheng-Li K, Huang Y, Rong W, Jia L. A polyacrylamide gel phantom for radiofrequency ablation. Int J Hyperthermia. 2008;24(7):568-76.
29. Itoi T, Isayama H, Sofuni A, Itokawa F, Tamura M, Watanabe Y, et al. Evaluation of effects of a novel endoscopically applied radiofrequency

ablation biliary catheter using an ex-vivo pig liver. J Hepatobiliary Pancreat Sci. 2012;19(5):543-7.

30. Steel AW, Postgate AJ, Khorsandi S, Nicholls J, Jiao L, Vlavianos P, et al. Endoscopically applied radiofrequency ablation appears to be safe in the treatment of malignant biliary obstruction. Gastrointest Endosc. 2011;73(1):149-53.
31. Goldberg SN, Ryan TP, Hahn PF, Schima W, Dawson SL, Lawes KR, et al. Transluminal radiofrequency tissue ablation with use of metallic stents. J Vasc Interv Radiol. 1997;8(5):835-43.
32. Pai M, Valek V, Tomas A, Doros A, Quaretti P, Golfieri R, et al. Percutaneous intraductal radiofrequency ablation for clearance of occluded metal stent in malignant biliary obstruction: feasibility and early results. Cardiovasc Intervent Radiol. 2014;37(1):235-40.

국문 초록

서론: 고주파 열치료(radiofrequency ablation, RFA)는 간세포암과 고도 이형성이 동반된 바레트 식도의 치료에 효과가 있는 것으로 알려져 있다. 근래에 담관 RFA 를 위한 양극성 RFA 카테터가 개발되었다. RFA 는 수술을 받기 어려운 간외 담관암 환자의 생존을 증가시킬 가능성이 있으며, 수술적 치료가 불가능한 악성 담관 폐쇄의 치료에 사용되는 자가 팽창성 금속 스텐트(self-expandable metal stent, SEMS)의 개존 기간을 연장할 가능성이 있다. 본 연구의 목표는 사용 전력에 따른 양극성 담관 RFA 의 효과를 정상 및 SEMS 삽입 돼지 담관에서 확인하고, 폴리아크릴아미드 겔 모형을 이용하여 SEMS 삽입 후 조직 내성장이 발생한 악성 담관 폐쇄에서 양극성 RFA 의 효과를 시뮬레이션하고자 하였다.

방법: 총 6 마리의 돼지를 사용하였다(정상 담관 RFA 3 마리, 비피막형 SEMS 를 삽입한 담관 RFA 3 마리). 전신 마취 후, 중간선 개복술을 시행하여 복강내에서 십이지장을 확인한 후, 십이지장을 절개하여 담관 개구부를 확인하였다. 정상 돼지 담관의 RFA 방법은 다음과 같다. RFA 카테터를 담관 입구에서 역행성으로 진행시킨 후, 돼지 한 마리 당 서로 다른 세 부위(근위부/중간부/원위부 담관)에 대해 동일한 전력으로 90 초간 RFA 를 시행하였다. 돼지별로 각각 5 W, 7 W, 10 W 의 전력으로 RFA 를 시행하였다. SEMS 를 삽입한 돼지 담관의 RFA 방법은 다음과 같다. 담관 개구부 확인 후 담관 내에

비피막형 SEMS 를 삽입하였다. SEMS 내강 내로 RFA 카테터를 진입시킨 후 세 마리의 돼지에 대해 RFA 를 10 W 의 전력으로 90 초 간 한 위치에만 시행하였다. 시술 후 실험 동물들을 안락사한 후, 담관을 절제하였으며, 절제된 담관에 대해 병리학적 검사를 통하여 응고괴사의 범위를 평가하였다. 또한 비피막형 SEMS 와 피막형 SEMS 를 넣은 폴리아크릴아미드 겔 모형을 제작한 후 10 W 의 전력으로 30 초 간 RFA 를 시행하여 RFA 의 범위를 평가하였다.

결과: 정상 돼지 담관의 RFA 깊이는 5 W, 7 W, 10 W 에서 각각 0.9 ± 0.3, 1.5 ± 0.2, 2.3 ± 0.6 mm 였다(analysis of variance; P = 0.02). RFA 전력과 RFA 깊이 사이에는 선형 관계가 있었다 (r^2 = 0.78; P = 0.003). SEMS 를 삽입한 돼지 담관에서는 RFA 의 범위가 RFA 카테터의 전극 사이에 국한되었으며, 10 W 의 전력에서 RFA 의 깊이는 점막 표면에 국한되었다. 비피막형 SEMS 를 넣은 폴리아크릴아미드 겔 모형에 대해 RFA 를 시행했을 때에는 응고 부위가 SEMS 에 닿자 전원의 차단이 발생하였다. 손상된 피막형 SEMS 를 넣은 폴리아크릴아미드 겔 모형에 대해 RFA 를 시행하였을 때에는 전원의 조기 차단은 발생하지 않았다. 10 개의 겔 모형 중 5 개에서 응고의 범위가 피막형 SEMS 내강내에 국한되었고, 나머지 5 개에서는 응고의 범위가 피막형 SEMS 의 벽 외부까지 확장되었다.

결론: 간외 담관암에서 양극성 RFA 치료는 비교적 안전하게 적용될 수 있을 것으로 생각된다. 그러나 비피막형 SEMS 내로 내성장한 종

양이 있으면 양극성 RFA 효과가 SEMS 내강 내에서도 각각의 전극 주변에 부분적으로만 발생하고, SEMS 밖으로는 미칠 수 없어서 효과가 떨어질 것으로 판단된다. 이와는 대조적으로 피막형 SEMS 내로 종양의 내성장이 발생한 경우에는 양극성 RFA 효과가 SEMS 내강뿐만 아니라 SEMS 밖으로도 어느 정도 미칠 수가 있어서 치료를 시도해 볼 수 있을 것으로 생각된다.

주요어: 카테터 절제법, 담관, 돼지, 금속 스텐트

학번: 2006-30512